PHYSICAL REVIEW B **72**, 201202(R) (2005)

Stress-induced platelet formation in silicon: A molecular dynamics study

J. G. Swadener, M. I. Baskes, and M. Nastasi
Materials Science and Technology Division, Los Alamos National Laboratory, Los Alamos, New Mexico 87545, USA
(Received 10 October 2005; published 30 November 2005)

The effect of stress on vacancy cluster configurations in silicon is examined using molecular dynamics. At zero pressure, the shape and stability of the vacancy clusters agrees with previous atomistic results. When stress is applied the orientation of small planar clusters changes to reduce the strain energy. The preferred orientation for the vacancy clusters under stress agrees with the experimentally observed orientations of hydrogen platelets in the high stress regions of hydrogen implanted silicon. These results suggest a theory for hydrogen platelet formation.

DOI: 10.1103/PhysRevB.72.201202 PACS number(s): 61.72.Tt, 61.46.+w, 68.55.Ln, 85.40.Ry

Vacancies are introduced into silicon in several processing steps during the production of semiconductor devices. Vacancies and vacancy clusters leave dangling bonds, which causes deep levels in the energy gap that act as carrier traps.[1,2] In addition, vacancies can act as traps for impurities and dopants or, in some cases, enhance their diffusivity. For monovacancies and some vacancy clusters, the structure and electronic properties are known from electron paramagnetic resonance or positron anihilation experiments or *ab initio* calculations.[1–12] However, not all signals and vacancy structures have been identified. Because vacancies have a significant effect on semiconductor properties, several studies have investigated the configurations of vacancy clusters.[13–20] However, the effect of stress on the structure of vacancy clusters has not been previously determined. Yet stress is usually present in layered silicon structures as are commonly used in semiconductor devices.

Vacancies are also thought to be important in hydrogen platelet formation, although the role of vacancies is still controversial. Several mechanisms have been proposed that involve an arrangement of vacancies as a precursor to hydrogen platelets,[21–24] while several other proposed mechanisms do not involve vacancy clusters.[25–28] Since hydrogen is also ubiquitous in silicon processing, its presence alone or in combination with vacancies can lead to deleterious effects on silicon device performance. Alternatively, hydrogen platelets can also be intentionally created for utilization in the commercially important ion cut process. In the ion cut process, H ions are usually implanted into a silicon wafer which creates residual in-plane compressive stresses in the wafer. Because stress is commonly present in several important silicon applications, we have investigated the effect of stress on vacancy clusters and platelet formation.

Our investigation uses molecular dynamics (MD) with a Si potential derived using the modified embedded atom method (MEAM).[29] The original MEAM Si potential[30] gave a relaxed vacancy formation energy of 2.84 eV, which is below experimental values (Watkins *et al.*[31] give 3.6±0.5 eV and Dannafaer *et al.*[32] give 3.6±0.2 eV) and *ab initio* calculations (3.5 eV–4.1 eV, see Estreicher *et al.*[33]). Therefore the MEAM potential was modified: $\beta^{(1)}$ was changed from 5.5 to 4.8 and $t^{(1)}$ was changed from 3.13 to 2.75 (see Table I), which increased the relaxed vacancy formation energy to 3.40 eV. The elastic constants determined using the modified potential are $C_{11}=164$ GPa, $C_{12}=69.5$ GPa, and $C_{44}=86.3$ GPa, which are close to the original potential and experimental values ($C_{11}=165.7$ GPa, $C_{12}=63.9$ GPa, and $C_{44}=79.7$ GPa).[34] Surface energies given by the modified potential are 1.33 J/m^2 for the unreconstructed (111) surface, 1.56 J/m^2 for the unreconstructed (110) surface, and 2.0 J/m^2 for the 2×1 reconstructed (100) surface, which are still close to the range of experimental values [Gilman[35] gives 1.24 J/m^2 for the (111) surface; Jacodine[36] gives 1.23 J/m^2 for the (111) surface, 1.51 J/m^2 for the (110) surface, and 2.13 J/m^2 for the (100) surface].

A model containing approximately 32 000 atoms in a cube measuring 88 Å with periodic boundary conditions was used to determine the relaxed energy of various vacancy clusters. Energy was minimized using the conjugate gradient method. Calculations of the formation energy of vacancy clusters using a 44 Å cube (4000 atoms) were within 1% of the results of the 88 Å cube at zero pressure. However, when stress was applied, the long range stress fields from the clusters (up to 11 Å in diameter) interacted and the results were over 2% different for the 44 Å and 88 Å cube models in some cases. The results for the stressed 88 Å cube model were within 1% of a model using a 132 Å (110 000 atom) cube for selected cases that showed the worst agreement with the 44 Å cube.

Several configurations for vacancy clusters were studied, because previous results have shown significant variations in energy depending on the cluster configuration.[15–17] While there is general agreement that the lowest energy configurations results from minimization of the number of dangling bonds, for clusters containing more than 10 vacancies, there are multiple arrangements for the same minimal number of dangling bonds. Chadi and Chang[13] originally predicted the $V6$ ring and $V10$ adamantine structures would be stable. (The notation Vn is used to denote a vacancy cluster with n vacancies). The stability of these $V6$ and $V10$ structures was confirmed by *ab initio* calculations,[37] where stability is defined as the energy of a Vn cluster being lower than the average of the energies of a $V(n-1)$ cluster and a $V(n+1)$ cluster. For larger vacancy clusters, Akiyama *et al.*[17] report that certain configurations of $V17$, $V22$, $V26$, and $V35$ are also stable, based on tight binding (TB) calculations. TB calculations by Bongiorno *et al.*[16] agree that $V6$, $V10$, $V17$, $V22$, and $V35$ are stable, but find that $V25$ and $V29$ are also stable, while $V26$ is not. Calculations with our MEAM potential agree with Bongiorno *et al.*[16] that $V6$, $V10$, $V17$, $V22$, $V29$,

 ©2005 The American Physical Society

TABLE I. MEAM parameters: sublimation energy E^0 (eV), equilibrium nearest neighbor distance R^0 (Å), cutoff radius r_c (Å), distance at which partial screening begins c_{min} and ends c_{max} (Å), exponential decay factor α, and cubic term strength δ for the universal energy function, scaling factor for the embedding energy A, exponential decay factors for the atomic densities $\beta^{(i)}$, and weighting factors for the atomic densities $t^{(i)}$.

E^0	R^0	r_c	c_{min}	c_{max}	α	δ	A	$\beta^{(0)}$	$\beta^{(1)}$	$\beta^{(2)}$	$\beta^{(3)}$	$t^{(0)}$	$t^{(1)}$	$t^{(2)}$	$t^{(3)}$
4.630	2.35	4.0	2.0	2.8	4.87	0	1.0	4.4	4.9	5.5	5.5	1	2.25	4.47	−1.8

and $V35$ are stable. The MEAM results indicate that $V26$ is stable, but the difference between $V25$ and $V26$ stability is less than 0.1 eV, which is within the possible error of our calculations.

For small vacancy clusters, the configurations based on hexagonal ring clusters (HRCs) are found to be lowest in energy using MEAM, in agreement with TB results.[16,17] There are different possible configurations for HRC depending on how the hexagonal rings are combined. Our results find that the HRC oriented in (111) planes are lowest in energy at zero pressure up to $V22$, in agreement with TB results.[16,17] Examples of HRC configurations are shown in Fig. 1. For $V23$ and $V24$, the lowest energy configuration of the HRC changes to a three-dimensional configuration, while for $V25-V34$, nominally spherical clusters are preferable, in agreement with TB results.[16] For $V35$, the lowest energy configuration is the perfect tetrahedron (in agreement with Refs. 16 and 17), which is both a three-dimensional HRC and a spherical cluster. The relaxed formation energies calculated using the MEAM potential are compared to previous TB results in Fig. 2. The agreement of MEAM with TB results shown in Fig. 2 is particularly notable since Stillinger-Weber and Tersoff potentials were shown to give poor agreement,[15] and the environment-dependent interatomic potential also shows an inaccurate linear dependence for small spherical clusters.[19]

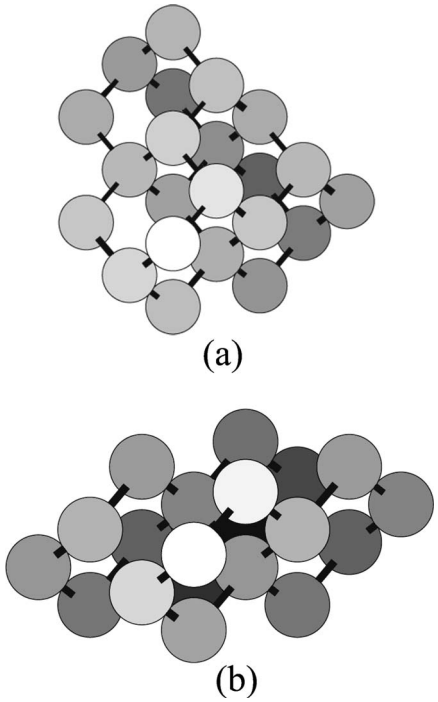

FIG. 1. Vacancy cluster configurations: (a) (111) planar HRC $V22$, (b) (100) planar HRC $V20$. Shading indicates depth.

In Fig. 3, the energy of formation for spherical clusters, (111) planar HRCs, and (100) planar HRCs at zero pressure are compared by taking the difference in the formation energy between the planar HRC and the spherical clusters of the same size. The results show that (100) planar vacancies have energies that are intermediate between the (111) planar vacancies and the spherical clusters for cluster sizes up to 20 vacancies. Planar HRCs at other orientations were higher in energy. Interestingly, the (111) planar HRC $V48$ is found to be 1.0 eV (0.02 eV per vacancy) lower in energy than the spherical $V48$. For clusters with 50 or more vacancies, the spherical clusters are lower in energy and the energy difference increases with the number of vacancies. Recently, Goss *et al.*[20] proposed that a (113) planar vacancy cluster would form in silicon, based on *ab initio* calculations for an infinite cluster with 1.0 eV per vacancy. However, we find that the (113) planar cluster is higher in energy. The (111) planar HRC $V72$ has a formation energy of 0.96 eV per vacancy and decreases to 0.53 eV per vacancy for an infinite (111) planar HRC. For spherical $V72$, the formation energy is 0.83 eV per vacancy, which decreases to 0.57 eV per vacancy for $V275$. Since the number of dangling bonds per vacancy continues to decrease for the spherical cluster, the formation energy per vacancy should continue to decrease with increasing cluster size.

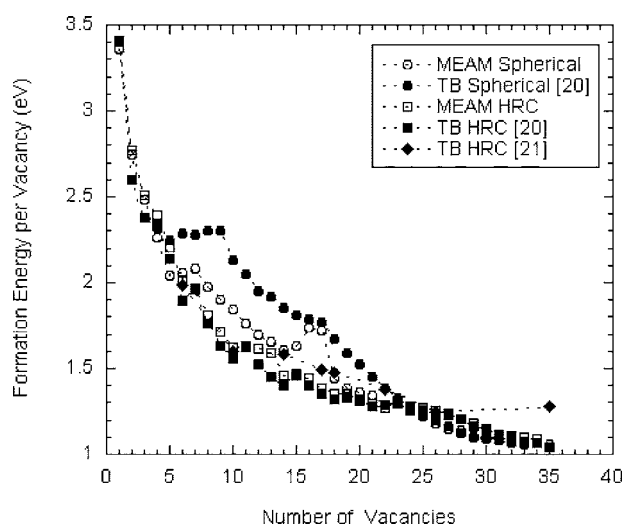

FIG. 2. Energy of formation per vacancy of vacancy clusters calculated using the MEAM potential for spherical clusters (open circles) and hexagonal ring clusters (HRC, open squares) compared to tight binding potentials by Bongiorno *et al.* (spherical clusters, full circles; HRC, full squares) (Ref. 20) and Akiyama *et al.* (Ref. 21) (HRC, full diamonds).

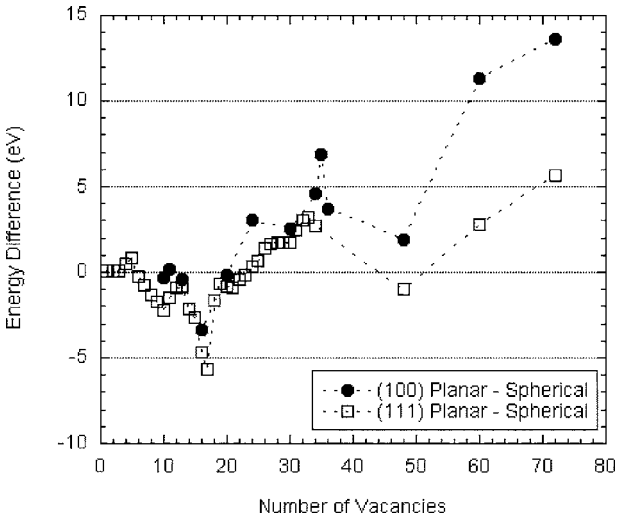

FIG. 3. Differences in total energy of formation between (100) planar HRC and spherical vacancy clusters (full circles), and between (111) planar HRC and spherical vacancy clusters (open squares) calculated using the MEAM potential at zero pressure.

Stress is found to have a significant effect on vacancy agglomeration. In order to reproduce the common stress conditions in layered silicon devices and in ion implanted silicon, a biaxial in-plane (compressive) strain of −0.01 was applied to the model and an out-of-plane tensile strain was applied to relieve the out-of-plane normal stress, resulting in a biaxial in-plane stress. When the biaxial compressive stress is applied in the (100) plane, (100) planar HRC become the lowest energy configuration for cluster sizes up to 20 vacancies. Figure 4 shows the difference in formation energy between the (100) and (111) planar HRC and spherical clusters under (100) biaxial compressive stress. For 22 or more vacancies, the spherical clusters are lowest in energy.

Two additional stress states were investigated. For biaxial compressive stress in the (111) plane, the results were similar to the unstressed case for biaxial in-plane strains of −0.01.

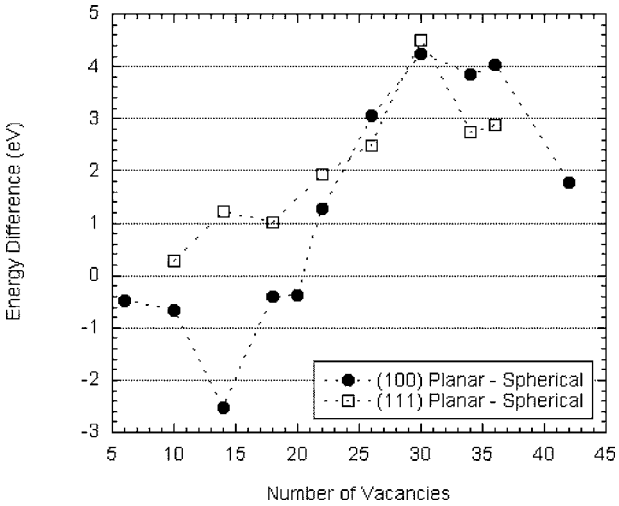

FIG. 4. Differences in total energy of formation between (100) planar HRC and spherical vacancy clusters (full circles), and between (111) planar HRC and spherical vacancy clusters (open squares) under biaxial compression in the (100) plane.

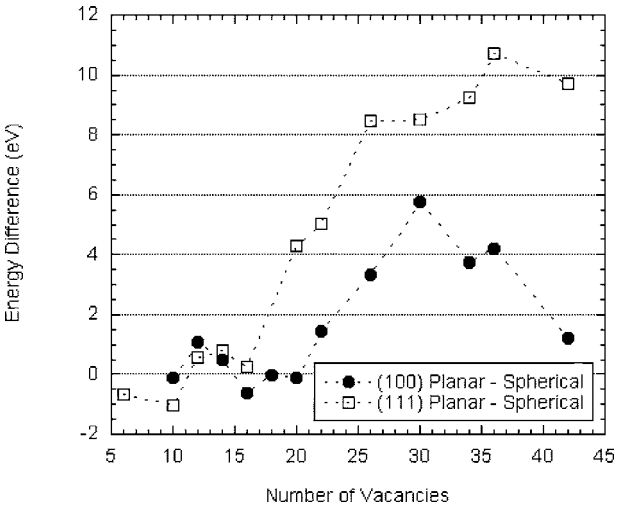

FIG. 5. Differences in total energy of formation between (100) planar HRC and spherical vacancy clusters (full circles), and between (111) planar HRC and spherical vacancy clusters (open squares) under biaxial compression in the (110) plane.

The (111) planar HRCs were lowest in energy for clusters up to 22 vacancies. When biaxial stress was applied in the (110) plane with an in-plane biaxial strain of −0.01, the results for the various configurations are compared in Fig. 5. The planar (111) HRCs are the lowest energy configuration only for clusters up to 10 vacancies. For $V12$ and $V14$, the spherical clusters are lowest in energy, while for 16–20 vacancies, the planar (100) HRC is lowest in energy. For larger clusters the spherical clusters are lowest in energy.

Experimental evidence of vacancy cluster configurations in silicon is limited to larger clusters of hundreds of vacancies, which are spherical. Clusters with fewer than 50 vacancies are probably too small for their structure to be definitively identified. Planar (100) vacancy clusters have been observed in SiGe layers that were under in-plane biaxial strain of −0.009.[38] Hydrogen platelets in the size range of 5–10 nm have been identified, but their structure is not completely determined because various contrast and underfocus or overfocus conditions can yield similar images for different structures.[39]

Based on our prediction that planar vacancies are stable only for small sizes, we propose that hydrogen platelets could be formed by a multistep process. First vacancies aggregate into small planar HRCs. The HRC could be oriented in (100) or (111) planes depending on the stress state. Second hydrogen atoms diffuse to the vacancy clusters and satisfy the dangling bonds on the cluster surfaces. Once the dangling bonds have been satisfied by the addition of hydrogen, the driving force for larger clusters to take a spherical shape would be eliminated. The platelets can then grow by Ostwald ripening or by the addition of free vacancies and hydrogen. The bonding energy of hydrogen to the surfaces of vacancy clusters has been found experimentally to give trapping energies of 1.4 and 1.7 eV per H,[40] apparently for bonding to two different locations or surfaces. For large (111) planar HRCs, the number of dangling bonds decreases to close to 0.5 per vacancy and the formation energy of the cluster decreases toward 0.53 eV per vacancy. Satisfying the dangling

bonds with hydrogen lowers the energy. Experiments indicate that the energy decrease is at least 0.7 eV per vacancy, which would result in a stable platelet. A large (100) planar HRC, while being approximately 40% higher in energy than the (111) planar HRC, has twice as many dangling bonds. Therefore the energy of (100) platelets will be lower than (111) platelets.

The stress-induced vacancy platelet model correctly accounts for some experimental observations that cannot be explained by existing models. Hydrogen platelets form at different orientations under different conditions. When hydrogen is introduced into silicon through diffusion or through a low energy plasma, where little or no stress is induced, (111) hydrogen platelets are formed. However, when hydrogen is implanted into (100) Si wafers, which induces a state of biaxial stress in the (100) plane, (100) platelets are formed in the region of highest stress at the center of implantation damage, while (111) platelets form in lower stress regions in the wafer.[41,42] Our model shows a possible explanation for the stressed-induced orientation in the growth of these platelets. In hydrogen implanted (111) Si wafers, where biaxial compressive stress is induced in the (111) plane, (111) platelets are formed in agreement with our model. In (110) Si wafers implanted with hydrogen, which induces biaxial compressive stress in the (110) plane, both (100) and (111) platelets are observed in the high stress region.[43] Our model predicts that (100) or (111) platelets could be formed, depending on the size the vacancy cluster reaches before hydrogen diffused in and satisfied the dangling bonds. Determining the numbers of (100) and (111) platelets that would be formed requires modeling of the kinetics of vacancy cluster growth and hydrogen diffusion, which is beyond the time scales accessible to the MD, but our model allows for the formation of both experimentally observed platelet orientations.

This research was funded by the U. S. Department of Energy, Office of Basic Energy Sciences.

[1] G. D. Watkins and J. W. Corbett, Phys. Rev. **138**, A543 (1965).
[2] G. D. Watkins, in *Deep Centers in Semiconductors*, edited by S. T. Pantelides (Gordon and Breach, New York, 1986), p. 147.
[3] M. Nisenoff and H. Y. Fan, Phys. Rev. **128**, 1605 (1962).
[4] W. Jung and G. S. Newell, Phys. Rev. **132**, 648 (1963).
[5] Y. H. Lee and J. W. Corbett, Phys. Rev. B **8**, 2810 (1973).
[6] M. Saito, A. Oshiyama, and S. Tanigawa, Phys. Rev. B **44**, 10601 (1991).
[7] Z. Tang, M. Hasegawa, T. Chiba, M. Saito, A. Kawasuso, Z. Q. Li, R. T. Fu, T. Akahane, Y. Kawazoe, and S. Yamaguchi, Phys. Rev. Lett. **78**, 2236 (1997).
[8] G. A. Baraff, E. O. Kane, and M. Schlüter, Phys. Rev. Lett. **43**, 956 (1979).
[9] R. Car, P. J. Kelly, A. Oshiyama, and S. T. Pantelides, Phys. Rev. Lett. **52**, 1814 (1984).
[10] O. Sugino and A. Oshiyama, Phys. Rev. Lett. **68**, 1858 (1992).
[11] P. E. Blöchl, E. Smargiassi, R. Car, D. B. Laks, W. Andreoni, and S. T. Pantelides, Phys. Rev. Lett. **70**, 2435 (1993).
[12] M. Saito and A. Oshiyama, Phys. Rev. Lett. **73**, 866 (1994).
[13] D. J. Chadi and K. J. Chang, Phys. Rev. B **38**, 1523 (1988).
[14] N. Cuendet, T. Halicioglu, and W. A. Tiler, Appl. Phys. Lett. **67**, 1063 (1995).
[15] L. Colombo, A. Bongiorno, and T. Diaz de la Rubia, in *Defects and Diffusion in Silicon Processing*, edited by S. Coffa, T. Diaz de la Rubia, P. A. Stolk, and C. S. Rafferty, MRS Symposia Proceedings No. 469 (Material Research Society, Pittsburgh, 1997), p. 205.
[16] A. Bongiorno, L. Colombo, and T. Diaz de la Rubia, Europhys. Lett. **43**, 695 (1998).
[17] T. Akiyama, A. Oshiyama, and O. Sugino, J. Phys. Soc. Jpn. **67**, 4110 (1998).
[18] A. La Magna, S. Coffa, and L. Colombo, Phys. Rev. Lett. **82**, 1720 (1999).
[19] M. Prasad and T. Sinno, Appl. Phys. Lett. **80**, 1951 (2002).
[20] J. P. Goss, P. R. Briddon, and R. Jones, J. Phys.: Condens. Matter **16**, 3311 (2004).
[21] P. Deák, C. R. Ortiz, L. C. Snyder, and J. W. Corbet, Physica B **170**, 223 (1991).
[22] M. A. Roberson and S. K. Estreicher, Phys. Rev. B **49**, 17040 (1994).
[23] M. K. Weldon *et al.*, J. Vac. Sci. Technol. B **15**, 1065 (1997).
[24] F. A. Reboredo, M. Ferconi, and S. T. Pantelides, Phys. Rev. Lett. **82**, 4870 (1999).
[25] P. Deák and L. C. Snyder, Radiat. Eff. Defects Solids **111–112**, 77 (1989).
[26] S. B. Zhang and W. B. Jackson, Phys. Rev. B **43**, R12142 (1991).
[27] S. Muto, S. Takeda, and M. Hirata, Philos. Mag. A **72**, 1057 (1995).
[28] Y.-S. Kim and K. J. Chang, Phys. Rev. Lett. **86**, 1773 (2001).
[29] M. I. Baskes, Phys. Rev. Lett. **59**, 2666 (1987).
[30] M. I. Baskes, Phys. Rev. B **46**, 2727 (1992).
[31] G. D. Watkins and J. W. Corbett, Phys. Rev. **134**, A1359 (1964).
[32] S. Dannefaer, P. Mascher, and D. Kerr, Phys. Rev. Lett. **56**, 2195 (1986).
[33] S. K. Estreicher, J. L. Hastings, and P. A. Fedders, Phys. Rev. B **57**, R12663 (1998).
[34] R. F. S. Hearmon, Adv. Phys. **40**, 323 (1956).
[35] J. J. Gilman, J. Appl. Phys. **31**, 2208 (1960).
[36] R. J. Jacodine, J. Electrochem. Soc. **110**, 524 (1963).
[37] A. Oshiyama, M. Saito, and O. Sugino, Appl. Surf. Sci. **85**, 239 (1995).
[38] P. I. Gaiduk, A. N. Larsen, J. L. Hansen, E. Wendler, and W. Wesch, Phys. Rev. B **67**, 235311 (2003).
[39] S. Muto, S. Takeda, and M. Hirata, Philos. Mag. A **72**, 1057 (1995).
[40] S. M. Myers, D. M. Follstaedt, H. J. Stein, and W. R. Wampler, Phys. Rev. B **45**, R3914 (1992).
[41] T. Höchbauer, A. Misra, M. Nastasi, and J. W. Meyer, J. Appl. Phys. **89**, 5980 (2001).
[42] M. Nastasi, T. Höchbauer, J. K. Lee, A. Misra J. P. Hirth, M. Ridgway, and T. Lafford, Appl. Phys. Lett. **86**, 154102 (2005).
[43] K. K. Bourdelle, T. Akatsu, N. Sousbie, F. Letertre, D. Delprat, E. Neyret, N. Ben Mohamed, G. Sucia, C. Lagahe-Blanchard, A. Beaumont, A.-M. Charvet, A.-M. Papon, N. Kernevez, C. Maleville, and C. Mazure, Proceedings of the 2004 IEEE International SOI Conference, 2004, p. 98.